



ISSN: 0976-3031

Available Online at <http://www.recentscientific.com>

CODEN: IJRSFP (USA)

International Journal of Recent Scientific Research  
Vol. 8, Issue, 10, pp. 20803-20809, October, 2017

**International Journal of  
Recent Scientific  
Research**

DOI: 10.24327/IJRSR

## Research Article

### CONTROLLED NANOCRYSTALLINE PRECIPITATION OF HYDROXYAPATITE ON THE SURFACE OF MICROFIBRILLATED CELLULOSE FIBERS

Kärner, K<sup>1\*</sup>, Elomaa, M<sup>1</sup>, Kallavus, U<sup>1</sup> and Tõnsuaadu, K<sup>2</sup>

<sup>1</sup>School of Engineering: Department of Mechanical and Industrial Engineering,  
Tallinn University of Technology, Estonia

<sup>2</sup>School of Engineering: Department of Materials and Environmental Technology:  
Tallinn University of Technology, Estonia

DOI: <http://dx.doi.org/10.24327/ijrsr.2017.0810.0963>

#### ARTICLE INFO

##### Article History:

Received 06<sup>th</sup> July, 2017

Received in revised form 14<sup>th</sup>  
August, 2017

Accepted 23<sup>rd</sup> September, 2017

Published online 28<sup>th</sup> October, 2017

##### Key Words:

BCTMP, bleached chemi-thermomechanical  
pulp, hydroxyapatite, wet chemical  
precipitation, SEM

#### ABSTRACT

In this study hydroxyapatite nanocrystals were synthesized on the surface of microfibrillated cellulose (MFC) fibers by using a wet chemical precipitation technique. MFC was prepared from bleached chemi-thermomechanical pulp (BCTMP) of aspen. KOH was used for pH regulation during apatite synthesis at 60 °C. Samples were dried under supercritical CO<sub>2</sub> and analyzed by scanning electron microscope (SEM). Measurements of surface area and surface charge, x-ray diffractometry and chemical analyses were performed. It was found that about 11 wt % of apatite is optimal dose for complete covering of the surface of MFC fibers. Synthesized apatite had Ca/P ratio of 1.6, which is (XRD) close to that of the stoichiometric ratio of hydroxyapatite.

**Copyright © Kärner, K et al, 2017**, this is an open-access article distributed under the terms of the Creative Commons Attribution License, which permits unrestricted use, distribution and reproduction in any medium, provided the original work is properly cited.

#### INTRODUCTION

Hydroxyapatite (HAp), also known as hydroxylapatite, Ca<sub>10</sub>(PO<sub>4</sub>)<sub>6</sub>(OH)<sub>2</sub>, is the major component of bone mineral and tooth enamel; it is an important inorganic material in biology and chemistry. HAp has outstanding properties concerning its medical uses. It is biocompatible, bioactive, non-toxic and non-inflammatory (Demirchan et al. 2012). That is why it has found applications in bone tissue engineering as well as in drug and gene delivery. Many other potential applications were reported basing to the absorptive properties of HAp. Those include absorption of CO (Nasr-Esfahani et al. 2012) and absorption of fluorine (Pandi et al. 2014).

Cellulose is the most abundant organic material and also an applicable material for making organic-inorganic hybrid materials. It is also known to be renewable, biodegradable and non-toxic (Klemm 2011). In recent years, cellulose-HAp composites have gained much attention. Cellulose-HAp composites have great potential for application in tissue engineering or bone regeneration. Cellulose and apatite mixtures have also been used for making scaffolds (Müller et al. 2006). Biomedical applications of HAp covered cellulose

use often bacterial cellulose (Nge et al. 2006, Zimmermann et al. 2011) or modified celluloses (Petrauskaitė et al. 2013) and bio-mimetic conditions for precipitations (Nge et al. 2006, Qu et al. 2012).

The most popular and widely explored technique for synthesis of HAp is the precipitation technique. This technique is also called as wet precipitation or chemical precipitation or aqueous precipitation and has chosen widely to synthesize HAp in contrast to other techniques (Nayak et al. 2010, Santos, et al. 2004, Markovic, et al. 2004). The important parameters for wet methods are pH (ranging from 6 to 11), temperature (ranging from room temperature to 200°C) maturation time and temperature. Composition and concentration of the reactants and their mixing rate are used to control the precipitation process (Santos et al. 2004, Ibrahim et al. 2000, Ferraz et al. 2004).

In our recent work was reported a partially nano-fibrillated cellulose product made of bleached chemo-thermo-mechanical pulp (BCTMP) (Kärner et al. 2016). Now our interest was to examine if that product is a suitable support for HAp. We know that our cellulose has negative surface charge (Kärner et al.

\*Corresponding author: Kärner, K

School of Engineering: Department of Mechanical and Industrial Engineering, Tallinn University of Technology, Estonia

2014) and high specific surface area. These two properties should be beneficial for growing HA on the material.

The electrokinetic properties of cellulose fibers are determined by the chemical composition of the fiber surface, the presence or absence of surface functional groups, the fiber porosity and the swelling behavior. Wood pulp fibers are negatively charged at all pH values due to the presence of acidic groups (carboxyl, sulphonic acid, phenolic or hydroxyl), which either derive from cell wall constituents or are introduced during pulping and bleaching of fibers.

HAp surface has both positive and negative ions such as  $\text{Ca}^{2+}$  and  $\text{PO}_4^{3-}$ , which can electrostatically bind with basic and acidic macromolecules (He *et al.* 2012) depending on the pH value of environment.

In cellulose the charged groups are located either on the fiber surface or inside the cell wall, therefore, they are referred to as surface and bulk charges. The number of charged groups depends on the origin of the fiber and on the chemical and mechanical treatment during pulping and refining. Surface charges influence the fiber-fiber bonding and interactions with high molecular mass additives. Surface charge of cellulosic fibers increases with increasing refining (beating) (Banavath, *et al.* 2011, Bhardwaj, *et al.* 2014, Bhardwaj, *et al.* 2006).

Hydroxyl groups are anionic functional groups with high affinity for  $\text{Ca}^{2+}$ . It has been stated that cellulose hydroxyl groups possess a strong negative dipole that could chelate free  $\text{Ca}^{2+}$  in the  $\text{CaCl}_2$  solution and form a coordinated bond, after which  $\text{PO}_4^{3-}$  could bond with the cellulose-associated calcium (Farbod, *et al.* 2014).

The concept of apatite formation on the bioactive materials generally includes twofold: the existence of the surface functional groups (hydroxyl and carboxyl groups in this study) that induce the heterogeneous nucleation of apatite, and the increased super saturation of the surrounding fluid that accelerates the nucleation process and growth (Nge *et al.* 2007).

It has been reported that calcium ions initiate a heterogeneous nucleation of HAp formation on the negatively charged surface (Morimune-Moriya, *et al.* 2015).

A well-known method for surface charge determination is polyelectrolytic titration; this method was pioneered by Terayama (Terayama *et al.* 1952) who determined the concentration of a cationic polyelectrolyte solution by titration with an anionic polyelectrolyte in the presence of a cationic indicator. Surface area of nanocellulose, as well as of nanoapatite, is strongly dependent on the drying methods and the solvent exchange. The latter gives surface areas about twice compared with regular freeze drying (Jin *et al.* 2004).

Many sophisticated works have been published about the covering of cellulose scaffolds with Hap (Petrauskaite *et al.* 2013, Zimmermann, *et al.* 2011, Wei, *et al.* 2004, Beladi *et al.* 2017). However, direct wet precipitation conditions are seldom used. In this study, MFC from BCTMP of aspen was prepared and different amounts of apatite were synthesized on the surface of cellulosic fibers. Our intention was to test how our aspen pulp based nano-fibrillated cellulose can be coated by

HAp. The whole process, including the production of MFC from BCTMP of aspen, was carried out in an environmentally friendly and cost-effective way. It was demonstrated that the deposition of HAp on aspen pulp derived nano-fibrillar cellulose is possible by a rather straightforward controlled nanocrystalline precipitation.

## MATERIALS AND METHODS

### Materials

Bleached chemo-thermo-mechanical pulp (BCTMP) of aspen was obtained from Estonian Cell. Aspen BCTMP was used as never-dried. NaOH, KOH, analytical grade urea and HCl were supplied from Sigma Aldrich and were used for chemical treatment of BCTMP. Polydiallyldimethylammoniumchloride (p-DADMAC) was used as cationic polyelectrolyte and potassium hydroxide (KOH) as titrant. P-DADMAC was supplied from Sigma Aldrich as a 20 wt% concentrate. Mw of p-DADMAC was 100000-200000 g/mol. Commercially available technical grade acetone with 99.5% purity from APChemicals was used in the solvent exchange process.  $\text{Ca}(\text{NO}_3)_2$ ,  $\text{H}_3\text{PO}_4$ ,  $\text{N}_2$ , He and ethanol were of laboratory grade. Ethanol [96.6 % vol] and acetone [95.5 % vol] were of laboratory grade and used without further purification. Commercially available technical grade  $\text{CO}_2$  with a purity of 99.7% from AGA was used in the supercritical  $\text{CO}_2$  drying process. Distilled water was readily used from the laboratory's own distilled water system.

### Equipment

For chemical pretreatment of BCTMP fibers commercially available disperser T 25 digit Ultra Turrax from IKA laboratory equipment was used. For mechanical treatment of MFC a vibration mill Narva Erbisard DDR- 6M9458 with glass balls with diameter of 10.2 mm were used. For apatite synthesis, Mettler Toledo T90 titrator was used as a pH controller and two Watson Marlow Sci 323 peristaltic pumps were used for calcium nitrate and phosphoric acid additions. Critical point drying was conducted in the Balzers apparatus. Mettler Toledo T90 titrator was used for surface charge measurements; it consists of a titrator with terminal, pH board, integrated burette drive and magnetic stirrer. It is expandable with two sensor boards (pH and/or conductivity) and up to seven additional burette drives (for dosing and titration purposes). For surface area measurements a sorptometer Kelvin 1042 built by Costech International was used. SEM studies were carried out with EVO MA 15 at accelerating voltage 12 to 15 keV. X-ray diffraction (XRD) patterns of cellulose and HAp were recorded by using a Rigaku Ultima IV diffractometer with monochromatic Cu  $K\alpha$  radiation ( $\lambda = 1.5406 \text{ \AA}$ , 40 kV at 40 mA). Data were gathered in the  $2\theta$  range of  $10^\circ$ - $50^\circ$  with scan speed of  $2^\circ/\text{min}$  and scan step  $0.02^\circ$  using the silicon strip detector D/teX Ultra. The X-ray diffractograms were analyzed using the software on the Rigaku system (PDXL 1.4.0.3).

### Methods

Microfibrillated cellulose from aspen wood pulp was obtained by using the same methodology as described in our previous article (Kärner, *et al.* 2015).

For apatite precipitation the  $\text{Ca}(\text{NO}_3)_2$  and  $\text{H}_3\text{PO}_4$  solutions (0.01 M) were added simultaneously into MFC-water slurry (0.1 L, pH=9.7) at rate of 2.0 and 1.2 ml/min, respectively, by peristaltic pumps, keeping Ca/P mole ratio equal to 1.67. The precipitation reaction can be written as:



pH of the synthesis environment was controlled by the titrator with electrode DG-112 Pro (pH stating using KOH 0.01M), calibrated with Mettler Toledo pH buffer solutions (4.01;7.00; 9.21) under  $\text{N}_2$  flow. The temperature was maintained at  $60 \pm 2$  °C. The obtained suspension was stirred for 1 hour at 60 °C and matured for 24 hours at room temperature. Apatite was precipitated in various concentrations; the concentration of apatite was controlled by the addition time of the solutions: 1 min, 2.5 min, 5 min and 10 min.

Ca and P content of the apatite samples were determined by standard analytical methods. Content of Ca was determined after thermal oxidation of MFC and dissolution of the residue in diluted HCl by AAS (Varian SpectrAA 55B Flame AAS) and phosphorus by photo colorimetry method as phosphomolybdate yellow complex (Biochrom Libras 70PC UV/Visible Spectrophotometer).

Apatite precipitation process on MFC is described in Figure 1.

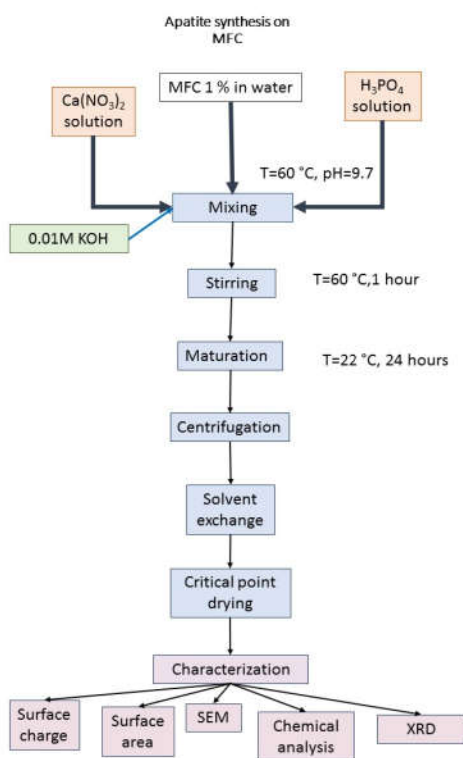


Figure 1 Apatite precipitation process and characterization methods

Surface charge was measured by using the same method as in our earlier work (Kärner *et al* 2013) by using 1 wt % p-DADMAC solution and 0.06 M KOH to find equivalence (end) point. After that surface charge was calculated according to Bhardwaj *et al*. 2006.

Specific surface area (SSA) measurement was performed using a Sorptometer KELVIN 1042. Helium was used as the carrier gas and nitrogen as the adsorptive gas. The specific surface area (SBET) was calculated according to the Brunauer-

Emmett-Teller (BET) theory. 0.02-0.06 g of MFC sample was degassed at 105 °C for 22 min to 169 min prior to the analysis followed by  $\text{N}_2$  adsorption at -196 °C. BET analysis was carried out for a relative vapor pressure of 0.01-0.3 at -196 °C.

## RESULTS AND DISCUSSION

Specifications of the samples are listed in Table 1. BCTMP of aspen was our initial sample without any treatment. MFC is chemically and mechanically treated BCTMP.

The results of specific surface area measurements can be seen from Figure 2. Apatite was precipitated on MFC samples 1 min, 2.5 min, 5 min and 10 min, leading to concentrations of 0.64 wt %, 1.32wt %, 3.4 wt% and 11.1 wt% of apatite respectively.

Table 1 Samples and their apatite contents

Sample	Sample name	Apatite concentration, weight%
1	BCTMP	0
2	MFC	0
3	MFC HAp 1 min	0.64
4	MFC HAp 2.5 min	1.32
5	MFC HAp 5 min	3.4
6	MFC HAp 10 min	11.1

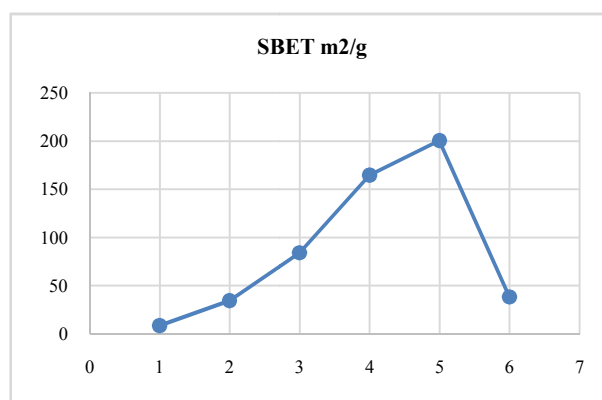


Figure 2 Surface area of MFC and apatite on MFC samples, listed in Table 1

The specific surface area determined by BET was 11.9-200.6  $\text{m}^2/\text{g}$ . Surface area value increases in the beginning of apatite precipitation due to additional surface between cellulose fibrils. As it can be seen from

Figure 2, surface area increased continuously until 5 min (3.4 wt %) of apatite precipitation. The maximum BET surface area value for MFC-HAp mixture (3.4 wt% HAp) was 201  $\text{m}^2/\text{g}$ .

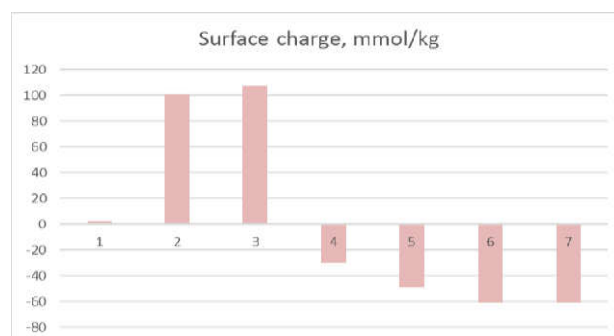


Figure 3 Surface charge of cellulose and apatite samples: 1) BCTMP, 2) chemically treated BCTMP, 3) MFC (chemically and mechanically treated BCTMP), 4) MFC with 1 min HAp precipitation; 5) MFC with 2.5 min HAp precipitation; 6) MFC with 5 min HAp precipitation; 7) MFC with 10 min HAp precipitation.

When the cellulose surface was totally covered by apatite (11%) the surface area value dropped.

Surface charge of MFC-apatite samples (Figure 4) is quite small for untreated BCTMP of aspen. However, it is in good correlation with our previous studies, where surface charge of initial sample (BCTMP) was also very low, 5.78 mmol/kg (Kärner, et al 2014).

An upsurge in the surface charge occurred after chemical treatment of BCTMP. The increase in surface charge continued after mechanical treatment. These were quite expected results, as there are more fine particles after chemical and mechanical treatment and they are responsible for higher surface charge values (Bhardwaj et al. 2006, Banavath, et al. 2011).

Surface charge decreased after adding of apatite, moreover, the charge turned negative and continued to decrease as apatite concentration increased. It can happen because of bonding of all available cellulose charged particles to apatite structure and carrying out the synthesis in basic environment (pH=9). Apatite itself has a negative charge, when pH is above 7. As our surface charge measurement method is not completely same as the conventional polyelectrolytic titration method (Horvath, et al. 2006, Bhardwaj et al. 2006, Banavath, et al. 2011), the results of surface charges measurements are specific only for the comparison of our samples.

The diffraction patterns of unmodified MFC, with precipitated and pure HAp are shown in Figure 3. Three peaks on curves a, b, and c at  $2\theta = 15.1, 16.7, 22.5$  deg confirmed that only cellulose I is present in the sample (Lu and Hsieh 2010), and the basic environment of HAp synthesis has not changed the crystalline structure of the sample. Weak characteristic to HAp (curve d) diffraction peaks at  $2\theta = 25.88, 31.88$  and  $40$  deg in curves b and c evidence the precipitation of HAp particles onto the surface of cellulose fibrillated structure (there was no any loose precipitated HAp particles in the reaction volume).

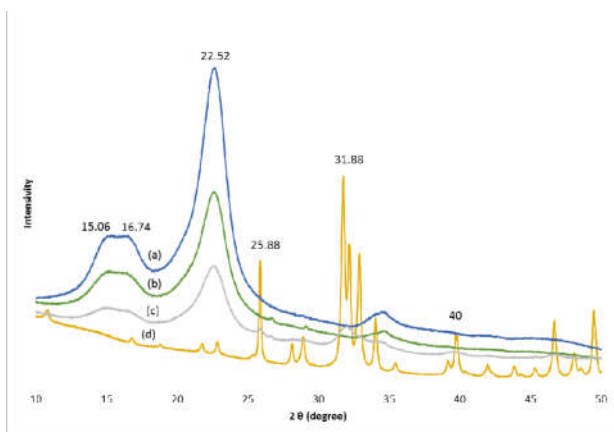


Figure 4 XRD of (a) starting MFC; (b) HAp 1min HAp precipitation; (c) HAp 10min HAp precipitation; (d) pure HAp

The chemical composition of precipitated HAp was calculated from the mean values of Ca and P contents. The calculated Ca/P molar ratio was 1.60, and is close to the stoichiometric value of 1.67.

Figure 5 shows the microstructure of initial sample, industrial BCTMP of aspen. It is a typical mechanical pulp showing diverse constituents of this kind of wood pulp. There are large

fibers as well as small particles: fines, fiber fragments, fibrils, lamellas. The most characteristic to any mechanical pulp is the presence of remnants of compound middle lamella easily recognizable by its rectangular shape. The surface of fibers is not showing particular fibrillation. For this sample the surface area and surface charge were both relatively small:  $8.6 \text{ m}^2/\text{g}$  and  $2.5 \text{ mmol}/\text{kg}$ , respectively.

In Figure 6 the microstructure of chemically and mechanically treated BCTMP microfibrillated cellulose is shown. There is much more of fine structure visible compared to BCTMP. Effective chemical and mechanical treatment liberated a part of remnants of compound middle lamella, primary wall and S1 layer exposing S2 layer of wood fiber with its characteristic parallel fibril orientation under a low angle toward fiber axis. Additionally, numerous fine fibrils have been released from the fiber's surfaces. The material is enough fibrillated to be a good starting point for precipitation of additives onto the MFC surface. Measurements of surface area and surface charge ( $34.5 \text{ m}^2/\text{g}$  and  $108 \text{ mmol}/\text{kg}$ , respectively) showed potential for a good bonding between fibers and other additives.

On the next figures (Fig. 7, 8, 9, 10) gradual attachment of HAp precipitated crystals is demonstrated. After 1 minute HAp precipitation (Fig.7) with the concentration of 0.64 wt %, the occurrence of HAp crystals is hardly visible and the crystals are very minute. Even though the concentration of apatite was relatively slow, surface area has increased to  $84.2 \text{ m}^2/\text{g}$ , but surface charge went slightly negative reaching the value of  $-30.4 \text{ mmol}/\text{kg}$ .

In the next Figure 8 when precipitation lasted for 2.5 min, numerous HAp crystals and agglomerates are visible attaching the surface quite regularly. HAp tends to form agglomerates rather than single crystals. The distance between apatite structures is about 200-300 nm, with crystal size approximately of 70 nm. Surface area has even more increased up to  $164.8 \text{ m}^2/\text{g}$ , but surface charge continued to drop to the value of  $-49.3 \text{ mmol}/\text{kg}$  (Fig.4).

The precipitation time of 5 min did not make major difference in the visible settlement of HAp crystals onto the surface of cellulose but the surface area continued to grow to the maximum value  $201 \text{ m}^2/\text{g}$ , and surface charge decreased continuously to the value of  $-60.9 \text{ mmol}/\text{kg}$ .

A drastic change occurred after 10 minutes of HAp precipitation onto the MFC (Figure 9).

The surface of MFC is totally covered with very thin but airy apatite layer. Apatite crystals and agglomerates were sparsely distributed covering the surface excellently. Airy layer formed due to the partially released but still attached to the surface nanofibrils of cellulose where HAp crystals and agglomerates were attached. After last precipitation experiment, surface area dropped sharply to the value of  $38.4 \text{ m}^2/\text{g}$  and surface charge remained almost the same compared with 5 minutes of apatite precipitation, to the value of  $-60.9 \text{ mmol}/\text{kg}$ .

This confirms that for our MFC product, 10 minutes of apatite precipitation is the optimum time to get primarily bound HAp crystals to make use of the surface charge of cellulose. It is not reasonable to add more apatite, because the active surface is already covered and further process will be as a sole

precipitation of apatite from the solution. It has been proved before, that there are accessible primary hydroxyl groups in cellulose that only take part in ion-ion reactions with HAp, the others (inaccessible hydroxyl groups) do not take part to it (Nge *et al.* 2006). It was shown in this experiment, that after 10 minutes of precipitation (11.1 wt % of HAp) those accessible hydroxyl groups were bonded with apatite, as the surface of MFC was totally covered with thin airy layer of HAp crystals. If the precipitation time is further increased, the apatite layers start to overlap with each other as there is no vacant area on MFC surface. It is also likely that some HAp might fall off from the surface. In all of our experiments, the maturation time after apatite precipitation was only 24 hours, therefore HAp crystals are not very large, longer time of maturation (as used earlier by Nge *et al.* 2006, Morimune-Moriya *et al.* 2015) would have probably caused bigger crystals.

## CONCLUSIONS

In this study, HAp was successfully incorporated into the MFC matrix by a wet chemical precipitation technique. Synthesized samples were characterized by using SEM, surface area and surface charge measurements, XRD and chemical analysis. Good bonding between apatite and cellulose surface was established. SEM micrographs showed that the precipitated HAp may consist of crystallites with the size of 1-1.5 $\mu\text{m}$ . To the end of experiment cellulose fibers were completely covered with fine airy layer of apatite crystals in 10 minutes (11.1 wt % of apatite). This can also be considered as optimal time or an amount as after that concentration apatite will not precipitate on the surface of cellulose but starts to form several apatite layers on top of each other. Surface charge was also small for initial sample, but started to increase after chemical and mechanical treatments.

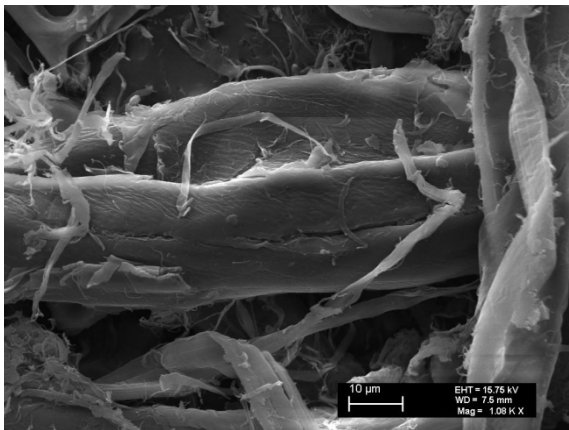


Figure 5 BCTMP

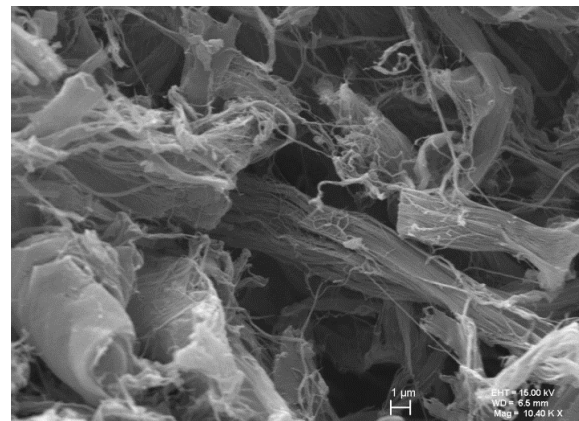


Figure 6 MFC

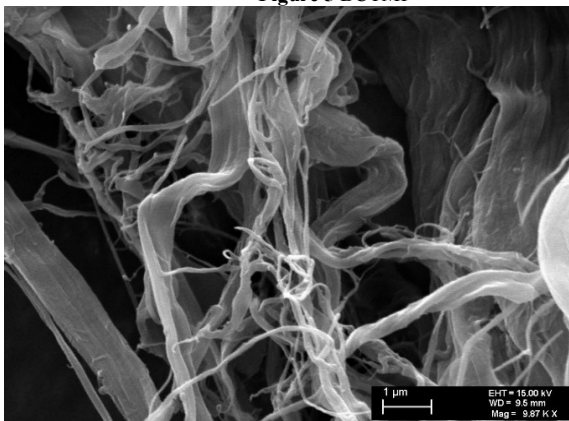


Figure 7 HAp 1 min

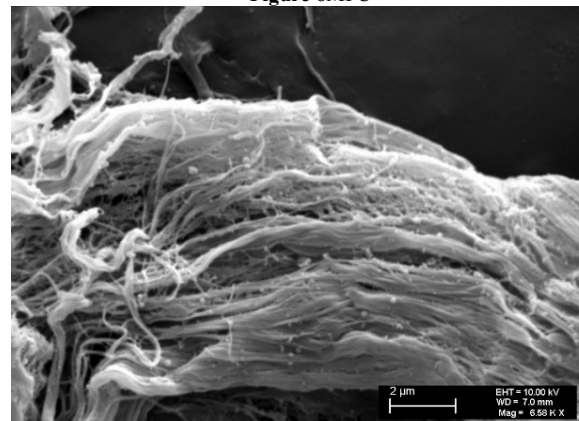


Figure 8 HAp 2.5 min

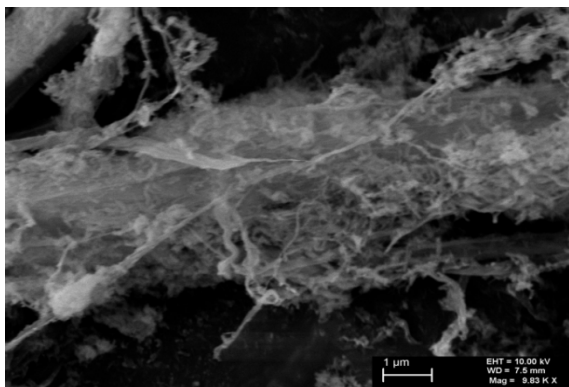


Figure 9 HAp 10 min

Surface charge of the samples with the precipitated HAp depend on the amount of apatite bound and dropped as the concentration of apatite increased.

XRD analyses showed that the crystallinity of cellulose did not change during the treatments. On grounds of the chemical analysis the formed apatite had a Ca/P ratio 1.6, which is close to stoichiometric hydroxyapatite (with Ca/P ratio 1.67).

The resulting material can be assumed to be potentially biocompatible, non-toxic, have interesting adsorption properties and economical price. However, further research is needed for assessment of possible applications.

## Acknowledgments

The authors would like to acknowledge the financial support of SmaCell project AR12138 and the Estonian Ministry of Education Science project IUT33-19. European Social Fund's Doctoral Studies and Internationalization Programme DoRa, which are carried out by Foundation Archimedes. A partial support from the projects IUT1-15 financed by Estonian Research Council is also acknowledged. Thanks are due to Dr. Arvo Mere (Department of Materials and Environmental Technology: Laboratory of Thin Film Chemical Technologies, TTU) and Dr. Mai Uibu (Laboratory of Inorganic Materials, TTU) for carrying out XRD and surface area measurements respectively.

## References

- Banavath, H. N., Bhardwaj, N. K., Ray, A. K. (2011). A comparative study of the effect of refining on charge of various pulps. *Bioresource Technology*, 102:4544-4551.
- Beladi, F., Saber-Samandari, S., Saber-Samandari S., (2017) Cellular compatibility of nanocomposite scaffolds based on hydroxyapatite entrapped in cellulose network for bone repair. *Materials Science and Engineering C* 75: 385-392.
- Bhardwaj, N. K., Hoang, V., Nguyen, K.L. (2006). Effect of refining on pulp surface charge accessible to polydadmac and FTIR characteristic bands of high yield kraft fibers. *Bioresource Technology*, 98:962-966.
- Brinkmann, A., Chen, M., Couillard M., Jakubek, J., Z., Leng, T., Johnson, L. J. (2016) Correlating Cellulose Nanoparticle Size and Surface Area, *Langmuir*, 32:6105-6114.
- A. C. Demirchan; V. S. Gshalaev, Editors, (2012) *Hydroxyapatite: synthesis, properties, and applications*. Hauppauge, New York.: Nova Science Publishers, Inc. Chapter IV, pp. 165-166.
- Farbod, K., Nejadnik, R., Jansen, J. A., Leeuwenburgh, S. C. G., (2014). Interactions between Inorganic and Organic Phases in Bone Tissue as a Source of Inspiration for Design of Novel Nanocomposites, *Tissue Engineering: Part B*, 20 (2):173-188.
- Ferraz, M. P., Monteiro, F. J., Manuel, C. M. (2004) Hydroxyapatite nanoparticles: A Review of Preparation Methodologies, *Journal of Applied Biomaterials & Biomechanics*, 2:74-80.
- He, M., Chang, C., Peng, N., Zhang, L., (2012) Structure and Properties of Hydroxyapatite/cellulose Nanocomposite Films, *Carbohydrate Polymers* 87:2512-2518.
- Ibrahim, D., M., Hegazy, W. H., Mahgoub, A. E., Abo-Elmaed, H. (2000) Preparation and Characterization of Calcium Hydroxyapatite, *Commun. Fac. Sci. Univ. Ank. Series B V*. 46:33-46.
- Horvath, E., Linström, T., Laine, J. (2006) On the indirect polyelectrolyte titration of cellulosic fibers. Conditions for charge stoichiometry and comparison with ESCA. *Langmuir*, 22(2):824-30.
- Jin, H., Nishiyama, Y., Wada, M., Kuga, S. (2004) Nanofibrillar Cellulose Aerogels, *Colloids and Surfaces A: Physicochemical Engineering Aspects* 240:63-67.
- Klemm, D., Kramer, F., Moritz, S., Tom Lindström, T., Mikael Ankerfors, M., Derek Gray, D., Annie Dorris, A. (2011) *Nanocelluloses Angewandte Chemie Int. Ed.*, 50: 5438 - 5466.
- Kärner, K.; Elomaa, M.; Kallavus, U. (2016). Fibrillation of Aspen by Alkaline Cold Pre-treatment and Vibration Milling. *Materials Science (Medžiagotyra)*, 22 (3): 358-363.
- Kärner, K.; Talviste, R.; Elomaa, M.; Kallavus, U. (2014). Study of the effect of mechanical treatment and supercritical CO<sub>2</sub> extraction on aspen BCTMP by surface charge measurements and SEM. *Cellulose Chemistry and Technology*, 48 (5-6): 535-544.
- Li, K., Lei, L., Camm, C. (2010) Surface Characterization and Surface Modification of Mechanical Pulp Fibres *Pulp & Paper Canada* January/February: 28 - 33.
- Markovic, M., Fowler, B. O., Tung, M.S. (2004) Preparation and Comprehensive Characterization of a Calcium Hydroxyapatite Reference Material, *Journal of the National Institute of Standards and Technology*, 109: 553-568.
- Lu, P., Hsieh, Y.-L. (2010) Preparation and Properties of Cellulose Nanocrystals: Rods, spheres, and Network, *Carbohydrate Polymers*, 82:329-336.
- Morimune-Moriya, S., Kondo, S., Sugawara-Narutaki, A., Nishimura, T., Kato, T., Ohtsuki, C., (2015), Hydroxyapatite Formation on Oxidized Cellulose Nanofibres in a Solution Mimicing Body Fluid, *Polymer Journal*, 47: 158-163.
- Müller, F. A., Müller, L., Hofmann, I., Greil, P., Wenzel, M. M., Staudenmaier, R. (2006), Cellulose-based Materials for Cartilage Tissue Engineering, *Biomaterials* 27: 3955-3963.
- Nasr-Esfahani, M.; Fekri, S. (2012). "Alumina/TiO<sub>2</sub>/hydroxyapatite interface nanostructure composite filters as efficient photo catalysts for the purification of air". *Reaction Kinetics, Mechanisms and Catalysis*. 107: 89-103.
- Nayak, A., K. (2010) Hydroxyapatite Synthesis Methodologies: An Overview, *International Journal of Chem Tech Research*, 2 (2): 903-907.
- Nge, T. T., Sugiyama, J., (2006) Surface Functional Group dependent Apatite Formation on Bacterial Cellulose Microfibrils Network in a Simulated Body Fluid, *Journal of Biomed Mater Res A*. 81(1):124-34.
- Pandi, K.; Viswanathan, N. (2014). "Synthesis of alginate bioencapsulated nano-hydroxyapatite composite for selective fluoride sorption". *Carbohydrate Polymers*. 112: 662-667.
- Qu, Ping; Zhang, Xiaoli; Zhou, Yitong; Yao, Siyu; Zhang, Liping. (2012) Biomimetic Synthesis of Hydroxyapatite on Cellulose Nanofibrils and Its Application *Science of Advanced Materials*, Volume 4, Number 2, February 2012: 187-192.
- Petrauskaitė, O., Gomes, de S., P., Fernandes, M. H., Juodzbalys, G., Stumbras, A., Maminskas, J., Liesiene, J., Cicciù, M. (2013) Biomimetic Mineralization on a Macroporous Cellulose-Based Matrix for Bone Regeneration. *Bio Med Research International*. Volume 2013:1-9.
- Santos, M.H., Oliviera, M., Souza, L. P., Mansur, H. S., Vasconcelos, W. L. (2004) Synthesis Control and

Characterization of Hydroxyapatite Prepared by Wet Precipitation Process *Materials Research* 7 (4): 625-630.  
Wei, G., Ma, P. X., (2004) Structure and Properties of Nano-hydroxyapatite/polymer composite scaffolds for Bone Tissue Engineering, *Biomaterials* 25: 4749-4757.

Zimmermann, K., LeBlanc, J., Sheets, K. T., Fox, W. R., Gatenholm, P., (2011) Biomimetic Design of a Bacterial Cellulose/Hydroxyapatite Nanocomposite for Bone Healing Applications, *Materials Science and Engineering C* 31:43-49.

**How to cite this article:**

Kärner, K *et al.* 2017, Controlled Nanocrystalline Precipitation of Hydroxyapatite on The Surface of Microfibrillated Cellulose Fibers. *Int J Recent Sci Res.* 8(10), pp. 20803-20809. DOI: <http://dx.doi.org/10.24327/ijrsr.2017.0810.0963>

\*\*\*\*\*